Ecotoxicology and Environmental Safety 236 (2022) 113486

Contents lists available at ScienceDirect

Ecotoxicology and Environmental Safety

journal homepage: www.elsevier.com/locate/ecoenv

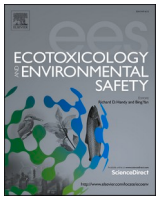

Potent necrosis effect of methanethiol mediated by METTL7B enzyme bioactivation mechanism in 16HBE cell

Jinting Lei [a], Guiying Li [a,b,*], Hang Yu [a,b], Taicheng An [a,b]

[a] Guangdong-Hong Kong-Macao Joint Laboratory for Contaminants Exposure and Health, Guangdong Key Laboratory of Environmental Catalysis and Health Risk Control, Institute of Environmental Health and Pollution control, Guangdong University of Technology, Guangzhou 510006, China
[b] Guangzhou Key Laboratory of Environmental Catalysis and Pollution Control, Key Laboratory of City Cluster Environmental Safety and Green Development (Department of Education), School of Environmental Science and Engineering, Guangdong University of Technology, Guangzhou 510006, China

ARTICLE INFO

Edited by Dr Yong Liang

Keywords:
Methanethiol
In vitro metabolism
Bioactivation
Cell necrosis
16HBE cells

ABSTRACT

Methanethiol is a widely existing malodorous pollutant with health effects on the human population. However, the cytotoxicity mechanism of methanethiol *in vitro* and its metabolic transformation (bioactivation or detoxification) have not been fully elucidated. Herein, the metabolites of methanethiol during cell culture and the cytotoxicity of methanethiol in human bronchial epithelial (16HBE) cells were investigated. Results indicate that methanethiol (10–50 μM) was partially converted into dimethyl sulfide, mainly catalyzed by thiol S-methyltransferase in the 16HBE cells, and then it induced potent cytotoxicity and cell membrane permeability. Moreover, methanethiol induced intracellular reactive oxygen species (ROS) up to 50 μM and further activated the tumor necrosis factor (TNF) signaling pathway, which eventually led to the decline in the mitochondrial membrane potential (MMP) and cell necrosis. However, all these effects were significantly alleviated with gene silencing of the methyltransferase-like protein 7B (METTL7B). These results indicate that methanethiol may induce cell necrosis in human respiratory tract cells mainly mediated by S-methyltransferase with interfering TNF and ROS induction. Non-target metabolomics results suggest that methanethiol potently affects expression of endogenous small molecule metabolites in 16HBE cells. To some extent, this work shows the possible conversion path and potential injury mechanism of human respiratory tract cells exposed to methanethiol.

1. Introduction

Malodorous sulfur-containing organic compounds are a group of chemicals with a low odor threshold that cause nausea and potential health risks to humans. They mainly include mercaptans, thioethers and carbonyl sulfide substances, and their representative substances include methanethiol, dimethyl sulfide, dimethyl disulfide and carbon disulfide (Tu et al., 2019; Yang et al., 2019). These kinds of compounds are mainly emitted during industrial processes, such as paper production (Singh and Chandra, 2019), solid waste landfilling (Lu et al., 2015; Yun et al., 2018), and kitchen waste anaerobic digestion (Zheng et al., 2020). For instance, 5–15,309 ng/g (dry matter) of methanethiol was detected in typical vegetable-fruit mixed waste (He et al., 2020); 8–36 μg/cm^3 dimethyl disulfide was detected in a hydrothermal hydrolysis unit of a food waste anaerobic digestion plant (Zheng et al., 2020); 0.065–0.35 mg/cm^3 dimethyl sulfide was detected in the headspace of a sewer (Sivret et al., 2016); and 87.6–457.3 mg/cm^3 dimethyl sulfide was detected in surface coastal waters of north China (Mao et al., 2021). A large number of studies suggest that methanethiol inhalation exposure causes a series of potential health risks, including dizziness; headache; vomiting; skin, eyes and heart irritation; severe respiratory paralysis; and even death (Fang et al., 2019; Jiang et al., 2021; Meng et al., 2019; Singh and Chandra, 2019). Although an understanding of the potential for respiratory diseases caused by methanethiol is emerging, the underlying metabolic mechanism and the exact signal pathway are unclear so far.

An *in vitro* study showed that 24 h exposure to 10 ng/mL methanethiol caused severe cytotoxicity and induced the proliferation of human gingival fibroblasts and periodontal ligament cells by inhibiting DNA synthesis in gingival fibroblasts (Johnson et al., 1992). Furthermore, it has been reported that volatile sulfur-containing organic compounds damage the integrity of the oral mucosa (Lancero et al., 1996). A

* Corresponding author at: Guangdong-Hong Kong-Macao Joint Laboratory for Contaminants Exposure and Health, Guangdong Key Laboratory of Environmental Catalysis and Health Risk Control, Institute of Environmental Health and Pollution control, Guangdong University of Technology, Guangzhou 510006, China.
E-mail address: ligy1999@gdut.edu.cn (G. Li).

https://doi.org/10.1016/j.ecoenv.2022.113486
Received 3 February 2022; Received in revised form 30 March 2022; Accepted 30 March 2022
Available online 6 April 2022

cute exposure (2 h) to methanethiol increased the permeability of the non-keratinized sublingual mucosa of pigs by 103% induction at 15 ng/mL level (Ng and Tonzetich, 1984). A respiratory exposure study showed an LC_{50} value of 675 ppm after 24 h exposure to methanethiol in adult Sprague-Dawley (SD) rats (Tansy et al., 1981). However, studying the toxicity of methanethiol to the human respiratory system has not been attempted yet and the mechanism remains unclear. Furthermore, methanethiol causes severe pulmonary toxicity, as it causes constriction of the terminal bronchioles, alveolar congestion and red blood cell exudation by induction of lipid peroxidation and apoptosis of lung epithelial cells, affecting the activity of antioxidant enzymes on SD rats. (Jiang et al., 2021). Moreover, other studies have shown that methanethiol has an inhibitory effect on cytochrome c oxidase (Waller, 1977), and also suppresses mitochondrial electron transfer in rat hepatocyte cells (Vahlkamp et al., 1979). However, the mechanisms of methanethiol-mediated mitochondrial damage and cell death have not yet been studied. Furthermore, the metabolic transformation mechanism of methanethiol as a malodorous air pollutant in respiratory tract cells is still not clear.

Thus, the present study was mainly designed to investigate the metabolic transformation mechanism of methanethiol, and the cell death signaling pathway in human bronchial epithelial (16HBE) cells was also explored using an *in vitro* methanethiol exposure model. This article mainly probed the metabolic transformation of methanethiol, and investigated the relationship between mitochondrial damage, intracellular reactive oxygen species (ROS) accumulation and cell necrosis caused by methanethiol. Furthermore, metabolomics was conducted to investigate the influence of methanethiol on endogenous small molecule metabolites in 16HBE cells. To some extent, this work addresses the inadequate information on the effects of malodorous pollutants on human respiratory tract cells.

2. Materials and methods

2.1. Chemicals

Methanethiol (10% in propanediol) was purchased from Macklin (Shanghai, China). N-Acetyl-L-cysteine (NAC, antioxidant) was obtained from MedChemExpress (MCE, Shanghai China). 2,7-Dichloro-dihydrofluorescein diacetate (DCFH-DA) and a Cell Counting Kit (CCK-8) were purchased from Dojindo (Tokyo, Japan). Annexin V-FITC, propidium iodide (PI), phosphate-buffered saline (PBS) and Hanks' balanced salt solution with calcium chloride and magnesium sulfate (HBSS/Ca/Mg) were purchased from Shenggong Biotech (Shanghai, China). Dulbecco's modified Eagle medium (DMEM), fetal bovine serum (FBS), penicillin, streptomycin and trypsin-EDTA (0.5%) were purchased from GIBCO (Thermo Fisher Scientific, MA, USA). RIPA lysis and extraction buffers were purchased from Thermo Fisher Scientific (MA, USA). The lactate dehydrogenase (LDH) cytotoxicity detection kit was purchased from TAKARA (Kyoto, Japan). Ebselen was purchased from Sigma-Aldrich and 4-methoxy-α-toluene mercaptan (internal standard) was purchased from TCI. A mmonium formate was purchased from CNW (Shanghai, China) and methanol (HPLC-grade) was purchased from Merck (Darmstadt, Germany). All other chemicals and reagents used in this study were of analytical grade.

Most antibodies were obtained from Cell Signaling Technology (Massachusetts, USA) and Abcam (Cambridge, UK), including rabbit antibodies recognizing human β-actin (cat.no. 8457S, 1:1000 dilution), RIP (cat.no. 3493T, 1:1000 dilution), phospho-CaMKII (12716T, 1:1000), MLKL (14993S, 1:1000), phospho-MLKL (91689S, 1:1000), PGAM5 (24584S, 1:1000), RIP3 (10188T, 1:1000), human methyltransferase-like protein 7B (METTL7B) (ab110134, 1:1000), cyclophilin 40 (ab181983, 1:10000), and mouse antibodies recognizing human CaMKII-α (cat. no. 50049S, 1:1000). The goat anti-rabbit IgG H&L (horseradish peroxidase (HRP)) (ab205718, 1:2000) and goat anti-mouse IgG H&L (HRP) (ab6789, 1:2000) were obtained from Abcam (Cambridge, UK).

2.2. Cell culture and exposure

The human bronchial epithelial (16HBE) cell line, obtained from the Chinese Academy of Cell Resource Center (Shanghai, China), was cultured in DMEM containing 10% FBS, 100 U/mL penicillin and 100 mg/mL streptomycin. Cell culture was carried out at 37 °C in a humidified atmosphere incubator containing 5% CO_2.

When the cell confluence reached 80%, the medium was replaced with fresh medium containing methanethiol, with the exposure concentrations set as 0, 10, 20, 30, 40 and 50 μM methanethiol. After 24 h exposure, the cell culture medium and cell pellets were respectively collected and used for further experiments.

2.3. Cytotoxicity determination

2.3.1. Cell viability and lactate dehydrogenase assay

The 16HBE cells were seeded in 96-well plates in full growth medium at a density of 1×10^4 cells/cm^2 (100 μL) and then placed in a humidified incubator with 5% CO_2 at 37 °C. Next, the cells were exposed to methanethiol for 24 h. After exposure, the cell medium was collected for detection of lactate dehydrogenase (LDH) release using the LDH cytotoxicity assay kit, and the cell pellets were used to determine cell viability with the CCK-8 Kit.

2.3.2. Determination of intracellular reactive oxygen species and mitochondrial membrane potential

Determination of intracellular reactive oxygen species (ROS) and mitochondrial membrane potential (MMP) was performed as previously described (Lu et al., 2021; Sun et al., 2021). That is, the 16HBE cells were plated in 96-well plates and cultured in DMEM. After being exposed to methanethiol and NAC, the supernatant of each well was removed, and the cells were washed twice with PBS. The intracellular ROS and MMP were determined using a ROS assay kit (Highly Sensitive DCFH-DA) and an MMP assay kit with JC-1, respectively.

2.3.3. Flow cytometric analysis for cell necrosis

The 16HBE cells were seeded in 6-well plates and exposed to methanethiol and NAC for 24 h. The cells were then washed with PBS and trypsinized. The density of the cells in each treatment was 5×10^5 cells/mL. The cells were resuspended in 195 μL binding buffer and 5 μL annexin V-FITC, and then incubated at room temperature for 15 min. The cells were washed and centrifuged at 94g for 5 min. Finally, the cells were resuspended in 190 μL binding buffer and 10 μL propidium iodide, and then analyzed using a BD FACSAria™ III flow cytometer within 4 h.

2.4. Cell transfection

METTL7B small interfering RNA (siRNA) and the negative control (NC) were obtained from RIBOBIO (Guangzhou, China). The target sequences of the siRNA were as follows: METTL7B_001 (siRNA-1) GAACCGGAGCCAACTTTCA, METTL7B_002 (siRNA-2) GAACAGGCACCTCCAATAT, and METTL7B_003 (siRNA-3) TCTCCGAAATCCAAATGGA. The detailed procedures of cell transfection are described in previous studies (Maldonato et al., 2021; Xiong et al., 2021; Ye et al., 2019). Briefly, cells were seeded in a 6-well plate (5×10^5 cells per well) and transfected with siRNAs and NC dissolved in lipofectamine 2000 (Invitrogen). After 72 h transfection, cells were collected for Western blot analysis.

2.5. RNA extraction, RT-qPCR and Western Blot

Total RNA extraction from the 16HBE cells was performed using Trizol (Life Technologies, USA). The RNA content of the samples was quantified by measuring the absorbance at 260 nm/280 nm and 260

nm/230 nm using a NanoDrop™ One/One^C Microvolume UV-Vis Spectrophotometer (Thermo Fisher Scientific, MA, USA). The qPCR volume was 20 μL, and the expression of β-actin was used as the internal reference. The entire process and the primer sequences are listed in Table S1 in the Supporting Information (SI). Total protein of the 16HBE cells was extracted using RIPA, and the protein concentration was analyzed using a BCA Protein Assay Kit (Pierce, Rockford, IL, USA). The extracted protein was separated by SDS-PAGE and then electro-transferred to polyvinylidene difluoride (PVDF) membranes (Millipore Corp, Atlanta, GA, USA). Subsequently, the membranes were blocked with 5% non-fat milk powder at room temperature for 2 h, incubated overnight with primary antibody at 4 °C, washed with PBS-T three times, and then incubated with HRP-conjugated secondary antibody at room temperature for 2 h. Finally, the signals of the bands were detected using electrochemiluminescence (ECL) reagents, and a chem-iluminescence instrument (Tanon5200) was used for imaging.

2.6. Detection of methanethiol and its metabolites in the culture media and headspace gas

2.6.1. Methanethiol and its metabolites in the culture media measured using UPLC-QTOF-MS

The 16HBE cells were cultured in 100 mm culture dishes under exposure to methanethiol for 2, 6, 10 and 24 h. Then, each cell culture medium sample was transferred to a 15-mL centrifuge tube, centrifuged at 845g at room temperature for 10 min to eliminate cell debris, and derivatized to avoid the volatilization of sulfides. The derivatization process was conducted as the work of predecessors (Vichi et al., 2013) and the derivatization principle is shown in Fig. S1 in the SI. To put it simply, 4 mL 0.01 mM Ebselen reagent, 5 μL internal standard (4-methoxybenzyl mercaptan) and 75 μL formic acid were added to the medium sample, which was then vortexed for 1 min, centrifuged at 845g for 10 min, and then the precipitate was discarded. Subsequently, the sample was aliquoted equally into two tubes, ultrapure water was added, and then HLB Pro SPE cartridges (60 mg, 3 mL/100 pcs) were used for desalination. The desalination process of the HLB Pro SPE cartridges is shown in the SI. After desalting, the sample was freeze-dried and, finally, 200 μL of pure methanol was used for reconstitution. The Agilent 1290 Infinity II Ultra-High-Performance Liquid Chromatography system coupled with a 6545 Quadrupole Time-of-Flight Mass Spectrometer (UPLC-QTOF-MS, Agilent, USA) was used for detection of methanethiol and its metabolites. The detailed procedure of the UPLC-QTOF-MS analysis is provided in the SI.

For non-targeted detection of metabolites in the cell culture medium, the related steps of the pre-processing methods and instrument parameters are shown in the SI.

2.6.2. Detection of methanethiol and its metabolites in the headspace gas using a gas chromatography-sulfur chemiluminescence detector

Methanethiol concentrations of 10 and 50 μM, which correspond to the low and high exposure concentrations to 16HBE cells, were selected for further analysis based on the results of the cell viability assay. The cells were cultured in 25 cm^2 culture flasks. The experiment consisted of a control group (cells with medium), a cell experiment group (cells plus medium and methanethiol), a cell-free negative control group (only medium and methanethiol), an si-RNA transfection group (cells plus medium and methanethiol, and siRNA-1), and an si-RNA negative control group (cells plus medium and methanethiol, and siRNA negative control). An Agilent 8890 GC with 8355 sulfur chemiluminescence detector (GC-SCD; Santa Clara, CA) was used to determine the volatile sulfur compounds in the headspace gas after exposure for 2, 6, 10, and 24 h. The headspace sample from the cell culture was injected in to the GC-SCD with a gas-phase injection needle. The volatile compounds were isolated using a DB-sulfur capillary column (60 m × 0.32 mm i.d., 4.2 μm film thickness; Agilent). Nitrogen was used as the carrier gas, and the flow rate was set to 2.8 mL/min. The inlet temperature was set to 150 °C, and the pressure was maintained at 17.3 psi. Sampling was performed in split mode, and the split ratio was 10:1. The oven temperature was kept at 35 °C for 3 min and then heated to 170 °C at a rate of 10 °C/min. For the Agilent 8355 SCD, the flow rates of hydrogen and air were set at 38 and 50 mL/min, respectively. The volatile sulfur compounds were identified on the basis of their retention times in relation to authentic standards.

2.7. Statistical analysis

All results presented in the current study represent at least three independent experiments and are expressed as the mean ± SD. One-way analysis of variance (ANOVA) was performed for statistical analyses using (SPSS 22.0) software, and a $p < 0.05$ is considered statistically significant.

3. Result and discussion

3.1. Methanethiol-induced cytotoxicity and necrosis of 16HBE cells

As shown in Fig. 1a, 24 h exposure to 10–30 μM methanethiol did not significantly induce cytotoxicity in 16HBE cells; however, a significant reduction of cell viability was observed at methanethiol concentrations ranging from 30 to 50 μM, as cell viability sharply decreased by 21.0% from 92.6%. The LDH activity increased from 46.8 to 73.5 U/mg protein under 10–50 μM methanethiol exposure, showing a concentration-dependent effect (Fig. 1b). In addition, after exposure to 10, 20 and 30 μM methanethiol, intracellular ROS increased by 1.8%, 3.1% and 11.4%, respectively, as compared with the control group, whereas exposure to 40 and 50 μM methanethiol increased the intracellular ROS by 1.5-fold and 1.6-fold compared with the control group (Fig. 1c). According to the flow cytometry results (Fig. S2 in SI and 1d), it can be found that methanethiol concentrations ranging from 10–50 μM all induced significant cell necrosis. This shows that methanethiol is cytotoxic to 16HBE cells, and could cause the production of intracellular ROS, possibly leading to the rupture of cell membranes at a certain concentration.

As shown in Fig. 2a, 24 h methanethiol exposure caused the up-regulation of genes in the cell necrosis pathway, confirming that methanethiol has the potential to cause cell necrosis. The tumor necrosis factor (TNF) gene was notably (more than 4.5-fold) up-regulated under high-concentration (50 μM) methanethiol exposure. Its receptor gene, TNF receptor superfamily member 1 A (TNFR1), increased by almost 2 times compared with the control group. Furthermore, receptor-interacting protein kinase 3 (RIPK3) showed a 2.2-fold up-regulation under 50 μM methanethiol exposure relative to the control group. These results suggest that methanethiol stimulates the expression of related genes in the cell necrosis pathway.

Intracellular MMP is regulated by the mitochondrial permeability transition pore (MPTP) (Halestrap et al., 2002), which is mainly composed of the proteins adenine nucleotide translocase (ANT), cyclophilin D (CypD) and voltage-dependent anion channel (VDAC) (Sinha and D'Silva, 2014). The results of this study show that methanethiol (50 μM) statistically induced mRNA expression of the ANT, CypD, VDAC and PGAM family member 5 (PGAM5) genes by 1.9-, 2.3-, 1.3- and 2.2-fold, respectively (Fig. 2a). More importantly, methanethiol caused damage to the MMP of the 16HBE cells, as reflected by the decrease in fluorescence intensity from 1.65 (10 μM) to 1.44 (50 μM), while the MMP was rescued to 1.52 under NAC co-exposure (Fig. 2c). This result is consistent with that of previous research and indicates that the reduction of MMP by methanethiol is associated with ROS (Liu et al., 2021). To further verify whether methanethiol-mediated ROS induction was the main cause of 16HBE cell necrosis, rescue experiments were performed by co-exposure to methanethiol and 1 mM NAC. Although the content of ROS labeled with fluorescent probes decreased by 18.1% when co-exposed with NAC (as compared with exposure to only 50 μM

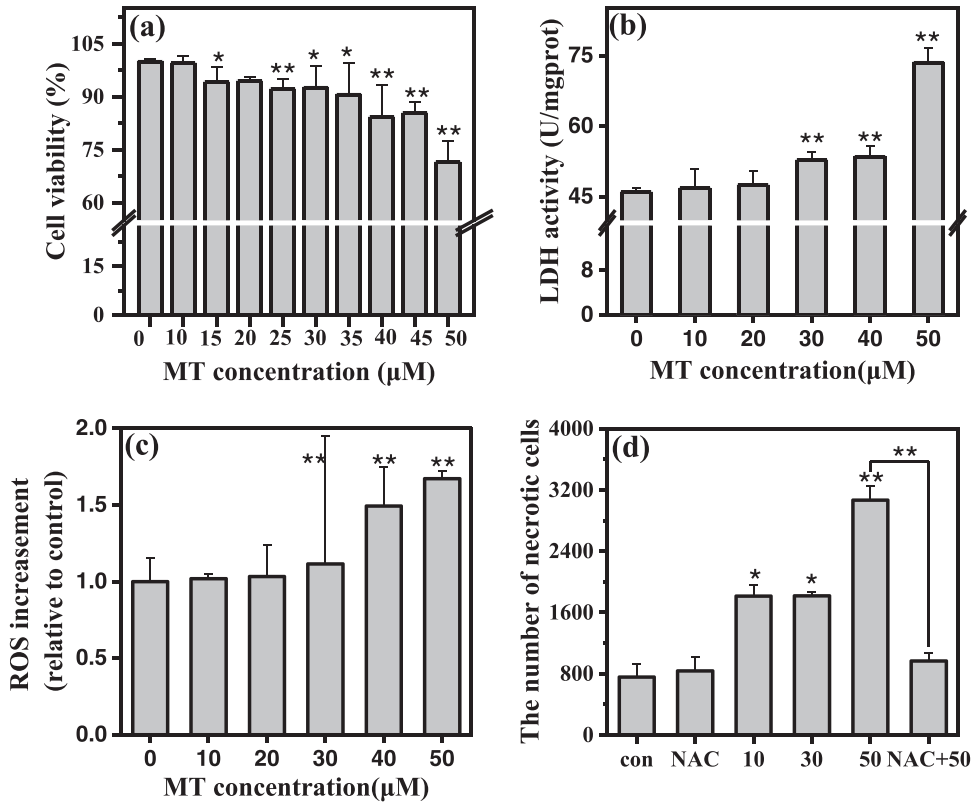

Fig. 1. Methanethiol induced cytotoxicity in 16HBE cells with 24 h exposure. (a) 16HBE cell viability. (b) LDH activity in the cell medium. (c) The increasement of ROS in cells. (d) Cell necrosis measured by flow cytometry. Data are presented as the mean ± SD. One-way ANOVA was used for the statistical analyses and $^{*}p < 0.05$, $^{**}p < 0.01$, n = 6, compared with control group.

methanethiol), it was still higher than that of the control group (Fig. 2b and S3). This result demonstrates that NAC can only partially inhibit methanethiol-mediated ROS generation in the 16HBE cells. Furthermore, the cell necrosis efficiency decreased by 44.5% (Fig. 1d), while the cell viability increased by 29.3% (Fig. S3) after co-exposure with NAC. Therefore, co-exposure with NAC could not only partially recover the methanethiol-mediated mitochondrial damage, but also act in a protective role against cell toxicity. Herein, the TNF signal pathway in the methanethiol-induced 16HBE cells was activated by ROS. More importantly, the expression of CypD, PGAM5, RIPK1 and p-CaMK proteins decreased by 8.0%, 14.0%, 14.0% and 38.0%, respectively, when co-exposed with NAC (Fig. 2d). The inhibition of ROS under co-exposure conditions could subsequently reduce methanethiol-mediated MMP damage and expression of the necrosis pathway.

As mentioned above, we can confirm that methanethiol exposure induces ROS. Furthermore, a concentration-dependent pattern was observed for the expression of TNF pathways and ROS generation, and the expression of TNF and RIPK1/RIPK3 showed a positive correlation (Figs. 1c and 2a). A previous study showed that TNF signaling affects mitochondrial ROS production or ROS clearance mechanisms (Vandenabeele et al., 2010). Theoretically, death receptor activation and/or caspase inhibition-induced mitochondria-mediated ROS generation is mainly dependent on the RIPK1/RIPK3 kinase complex (Lin et al., 2004). Cho et al. found that RIP3 regulates the production of ROS during cell necrosis (Cho et al., 2009). Therefore, we further inferred that the production of ROS under methanethiol exposure may be regulated by TNF and RIPK3. The up-regulation of TNF, TNFR1, RIPK1 and RIPK3 in this study further demonstrates that methanethiol exposure can promote activation of the necrosis pathway. This is because TNF is an important cytokine that plays key physiological and pathological roles in cell necrosis and apoptosis (Chu, 2013; Vandenabeele et al., 2010). RIPK1 and RIPK3 are also important molecular switches in the cell necrosis pathway (Baines, 2010).

A large number of studies indicate that ROS plays an important role in the activation of cell signaling pathways (Fleury et al., 2002). The mitochondrial permeability conversion channel complex is mainly composed of the VDAC, ANT and CypD proteins (Baines, 2010). Among them, the CypD has been found to be a key MPTP-induced cell necrosis regulator that can regulate the opening and closing of MPTP (Festjens et al., 2006; Ying and Padanilam, 2016). The q-PCR analysis in this study shows that during the methanethiol exposure process, the expression of VDAC, ANT and CypD significantly increased (Fig. 2a). To a certain extent, we can infer that exposure of the 16HBE cells to methanethiol may activate CaMKII through the TNF pathway, leading to opening of the MPTP. This process may also be related to ROS, further leading to a decrease in the MMP and the appearance of cell necrosis. Intracellular ROS generation due to methanethiol exposure may play an important role in regulating downstream signaling molecules in the TNF signaling pathway, together leading to cell necrosis. In the TNF-induced cell necrosis pathway, ROS acts as a very important mediator (Blaser et al., 2016). Therefore, the production of ROS in the mitochondria is of great significance for cell stress signals and cell survival, which is closely related to the energy state of the cell, metabolite concentrations and other upstream signaling events. (Hamanaka and Chandel, 2010).

3.2. *Methanethiol metabolism catalyzed by METTL7B in 16HBE cells*

To explore the intermediates of cellular methanethiol biotransformation, metabolites in the cell culture medium and headspace gas were analyzed using UPLC-QTOFMS and GC-SCD, respectively. The methanethiol peak derivatized using Ebselen reagent was detected with an accurate mass of *m/z* 321.9810, and the derivatized internal standard compound was detected with a mass of *m/z* 428.0221. The total ion current diagram, extracted ion current diagram, and secondary mass

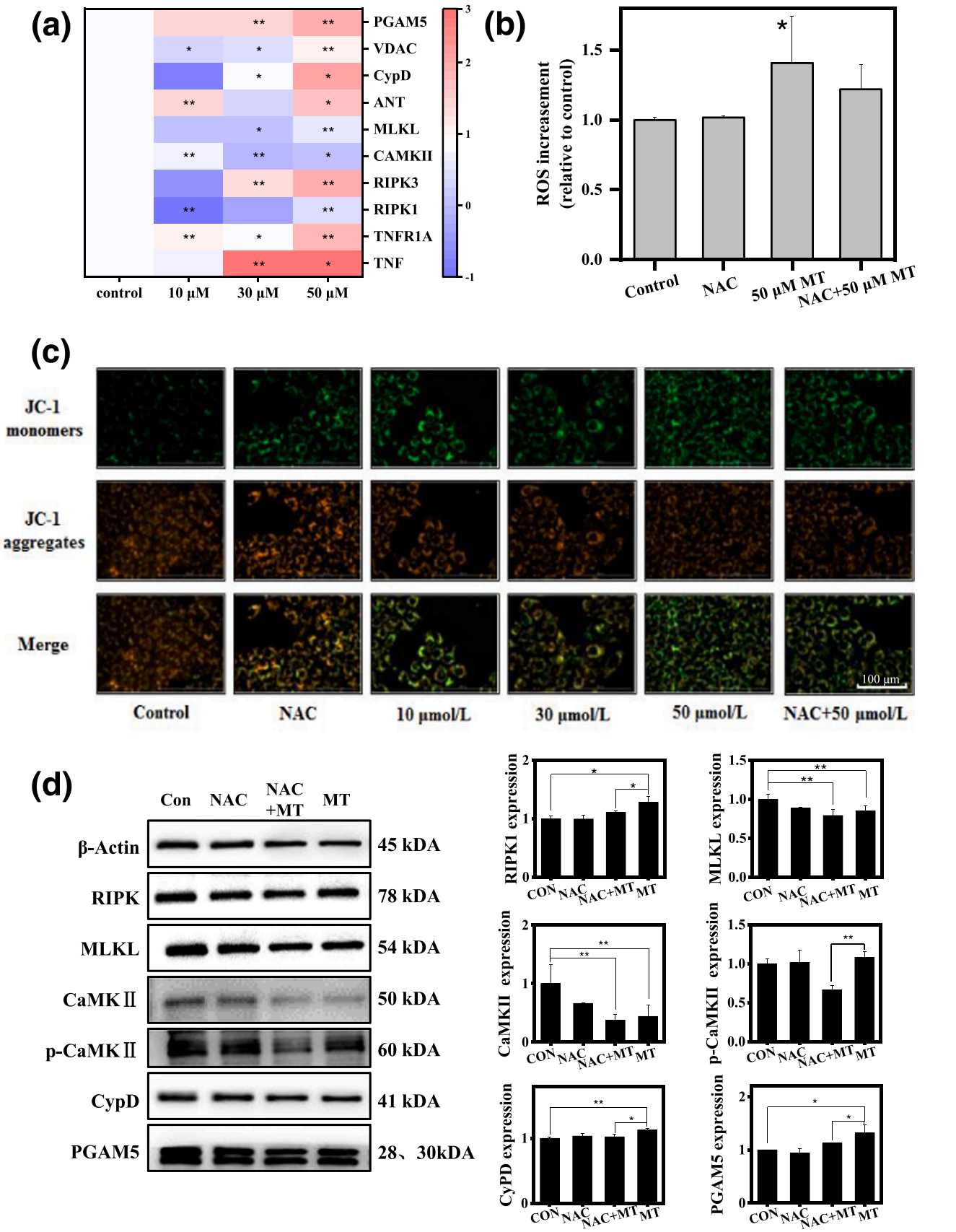

Fig. 2. Methanethiol induced MMP, related gene and protein expression in 16HBE cells, and the influence of NAC. (a) The mRNA expression of necrosis-related genes in TNF pathways. (b) The change of ROS, and influence of NAC. (c) The MMP detected by using live-cell imaging technology. (d) Expression of related proteins in cell necrosis pathways. Data are presented as the mean ± SD. One-way ANOVA was used for the statistical analyses and $*p < 0.05$, $**p < 0.01$, n = 6, compared with control group.

spectrum information of *m/z* 321.9810 are showed in the SI (Fig. S3). The extracted ion current of the derivatized product (*m/z* 321.9810) for the control group, the low-concentration group (10 μM) and the high-concentration group (50 μM) for 24 h exposure are shown in Fig. 3a. The internal standard method was used for quantitative determination of methanethiol, which represents the concentration of methanethiol in the cell culture medium. No derivatization metabolite (*m/z* 321.9810) was found in the control group. However, the decreased concentration of methanethiol in the cell culture showed a time-dependent pattern (Fig. 3a and b). Moreover, in the low-concentration exposure group (10 μM), the methanethiol concentration decreased from 0.47 to 0.05 mg/L within 24 h, and in the high-concentration exposure (50 μM), the methanethiol concentration decreased from 0.66 to 0.05 mg/L within 24 h (Fig. 3c). The methanethiol content rapidly decreased within 6 h and plateaued at about 10 h (Fig. 3c). The methanethiol metabolite dimethyl sulfide (DMS) could not be found in the extracted ion current diagram (Fig. S4), due to its strong volatility. Thus, we used the GC-SCD to directly detect DMS without derivatization via confirmation of the calibration curves of the standard sample (Fig. 3d). Therefore, using the combined data obtained via UPLC-QTOFMS and GC-SCD, we concluded that methanethiol is a substance that can be rapidly metabolized through cell metabolism, and most metabolites would be rapidly released into the headspace.

Generally, the composition and concentration of volatile substances in the headspace gas can reflect the cell metabolism process to a certain extent (Furuhashi et al., 2020; Liu et al., 2019). To investigate the metabolic transformation of methanethiol during cell exposure, the volatile intermediates in the headspace gas were measured using GC-SCD. The chromatogram results show that the retention times of these volatile compounds were 5.341, 8.067 and 14.377 mins (Fig. 3d), which represent methanethiol, DMS and dimethyl disulfide (DMDS), respectively, as validated by the standard gas sample. From Fig. 3d, we could conclude that trace amounts of three kinds of sulfides of interest were detected in the control group and the siRNA negative control (si-NC) group. DMS could only be detected in the presence of cells, while methanethiol and DMDS could be detected in the cell-free group. Furthermore, the response area of DMDS was generally larger than that of methanethiol, while the DMS concentration might have been lower than the detection limit. Therefore, DMDS might be produced by the interaction between methanethiol and the cell culture medium, or it may be produced by the oxidation of methanethiol itself (Yao et al., 2019). Conversely, DMS is produced by the intracellular metabolism of methanethiol.

Based on an early study (Bremer and Greenberg, 1961), we postulated that the thiol methyltransferase in the 16HBE cells may be involved in this methanethiol metabolic process. A recent study has shown that the human METTL7B performs very similar functions as thiol methyltransferase, and the authors even suggest that METL7B is probably a type of thiol methyltransferase (Maldonato et al., 2021). Therefore, in this work, the 16HBE cells were first transduced with METTL7B si-RNA and then the sulfide metabolism was measured in the headspace gas (expression of the knocked down METTL7B gene in the 16HBE cells is shown in Fig. S5). In the METTL7B knockdown group, the DMS response was significantly lower than that of the group exposed to 50 μM methanethiol (Table S2). Specifically, the concentrations of the three kinds of sulfides in the solution were quantitatively determined using the standard curve. Moreover, as the exposure time increased, the concentration of methanethiol and DMDS gradually decreased, while the concentration of DMS increased slightly in both the 10 and 50 μM methanethiol exposure groups (Table S2 in SI). Within 10 h, the methanethiol concentration decreased from 4.9 to 3.3 mg/L, DMDS decreased from 0.9 to 0.3 mg/L, and DMS increased from 0.08 to 0.68 mg/L under 10 μM methanethiol. After 10 h exposure to 50 μM methanethiol, a more substantial decrease in the concentrations of methanethiol (from 6.7 to 4.9 mg/L) and DMDS (from 2.9 to 1.3 mg/L) was observed, while DMS increased from 0.13 to 0.43 mg/L. The increase in the DMS concentration during methanethiol exposure indicates that DMS may be a metabolic conversion product of methanethiol accumulated in the 16HBE cells. After 24 h, the DMS content in the medium was 0.34 and 0.33 mg/L for the 10 and 50 μM methanethiol exposure groups, respectively. Comparatively, methanethiol was transformed to DMS only in the presence of 16HBE cells, whereas in the absence of cells, most of the methanethiol was transformed into DMDS. In the METTL7B knockdown group after 10 h exposure to 10 and 50 μM methanethiol, 0.2 and 0.1 mg/L of methanethiol were detected, respectively, while the DMDS concentrations reached 1.4 and 1.3 mg/L, respectively. Therefore, methanethiol might be converted into DMS in the presence of these cells. More importantly, in the si-RNA group, the concentrations of methanethiol, DMS and DMDS were all lower than those measured in the normal exposure group. Compared with the cells in the normal exposure group, the DMS concentration measured in the si-RNA group decreased by 0.23 and 0.04 mg/L after 10 h exposure at 10 and 50 μM methanethiol, respectively. This indicates that inhibition of METTL7B reduces the production of DMS to a certain extent, and that METTL7B participates in the biotransformation of methanethiol.

Regarding the metabolism and transformation of methanethiol *in vivo*, the metabolic intermediates of methanethiol have not been elucidated and the metabolic mechanism is still not clear; however, there are some reports related to rats and humans (Derr and Draves, 1983; Tangerman, 2009). Lake et al. studied the metabolism of furfuryl mercaptan and 2-methyl-3-furanthiol in the liver and blood of rats (Lake et al., 2003). The authors proposed that substances with a sulfhydryl structure will first be methylated at the sulfhydryl position, and then further oxidized into sulfoxide and sulfone. As with these two substances, methanethiol also has a sulfhydryl structure. Therefore, in this study, the presence of DMS in the headspace of the 16HBE cells was confirmed both by GC-SCD and UPLC-QTOFMS. From this, it was inferred that methanethiol will also first undergo methylation in the 16HBE cells, and then be oxidized to dimethyl sulfoxide and dimethyl sulfone. Importantly, we found that the volatile metabolic conversion product of methanethiol catalyzed by thiol methyltransferase in the 16HBE cells was DMS. Thiol methyltransferase (S-adenosyl-L-methionine: thiol S-methyltransferase, EC 2.1.1.9) is a type of transfer enzyme that can catalyze the transfer of methyl from S-adenosyl-methionine to S-adenosyl-homocysteine; that is, it can methylate exogenous sulfhydryl-containing compounds (e.g., mercaptoethanol) (Glauser et al., 1992) instead of physiological sulfhydryl-containing compounds (e.g., homocysteine, cysteine) (Borchardt and Cheng, 1978). A series of non-physiological sulfhydryl compounds (e.g., BAL, mercaptoethanol, O-methyl-mercaptoethanol, thioglycolic acid, fluoromercaptopropionic acid, methanethiol and hydrogen sulfide) have also been found to serve as methyl-accepting substrates (Bremer and Greenberg, 1961). However, the gene and protein sequences responsible for the activity of human thiol methyltransferase remains unknown. The latest research shows that METTL7B can catalyze the transfer of methyl groups from S-adenosyl-1-methionine to hydrogen sulfide and other small exogenous thiol molecules (Maldonato et al., 2021). Moreover, the partial inhibition of methanethiol metabolism in the 16HBE cells was also confirmed with the METTL7B knockdown experiment. As the expression of METTL7B in the 16HBE cells was detected in this study, we could speculate that methanethiol is methylated by METTL7B in 16HBE cells to form DMS.

3.3. The bioactivation and metabolomics effects of methanethiol in 16HBE cells

As METTL7B was knocked down by gene silencing, methanethiol metabolism in the cell was also found to be inhibited (Fig. 3d). Thus, methanethiol was converted into DMS by the catalyzation of METTL7B in the 16HBE cells. Fig. 4 compares the toxic effects of methanethiol before and after METL7B knockdown. As shown in Fig. 4a, the cell viability after si-RNA transfection was found to be reduced at the same exposure concentration compared with the group without gene

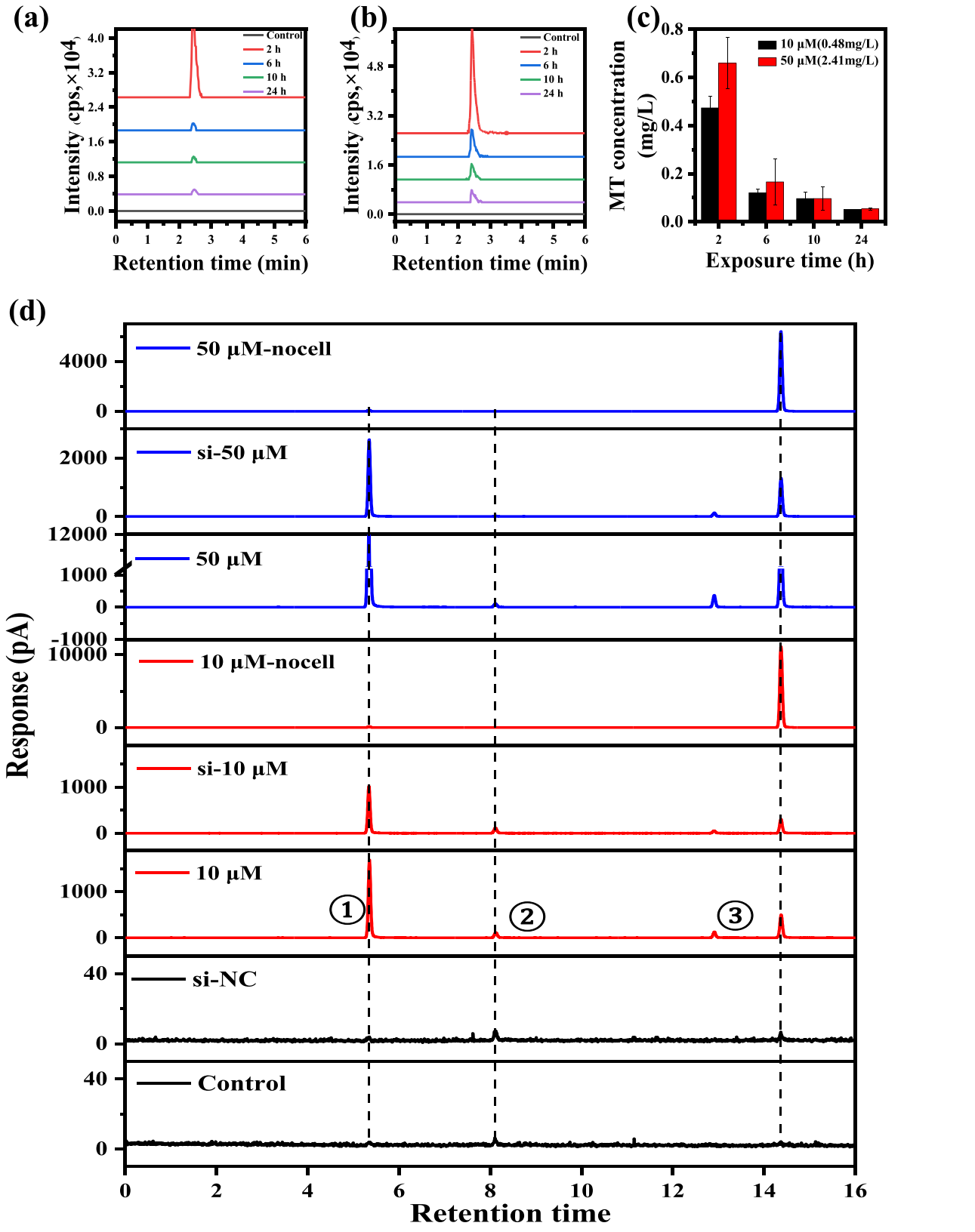

Fig. 3. Measurement of cell medium and headspace gas metabolites in 16HBE cells by UPLC-QTOF-MS and GC-SCD after exposure. Response of the peak area of *m/z* 321.9810 with different methanethiol exposure concentrations of 10 μM (a) and 50 μM (b) at different times. (c) The concentration of methanethiol in cell culture medium with different exposure times. (d) The corresponding area of ① methanethiol (MT), ② DMS, and ③ DMDS in the headspace gas measured by GC-SCD in different groups.

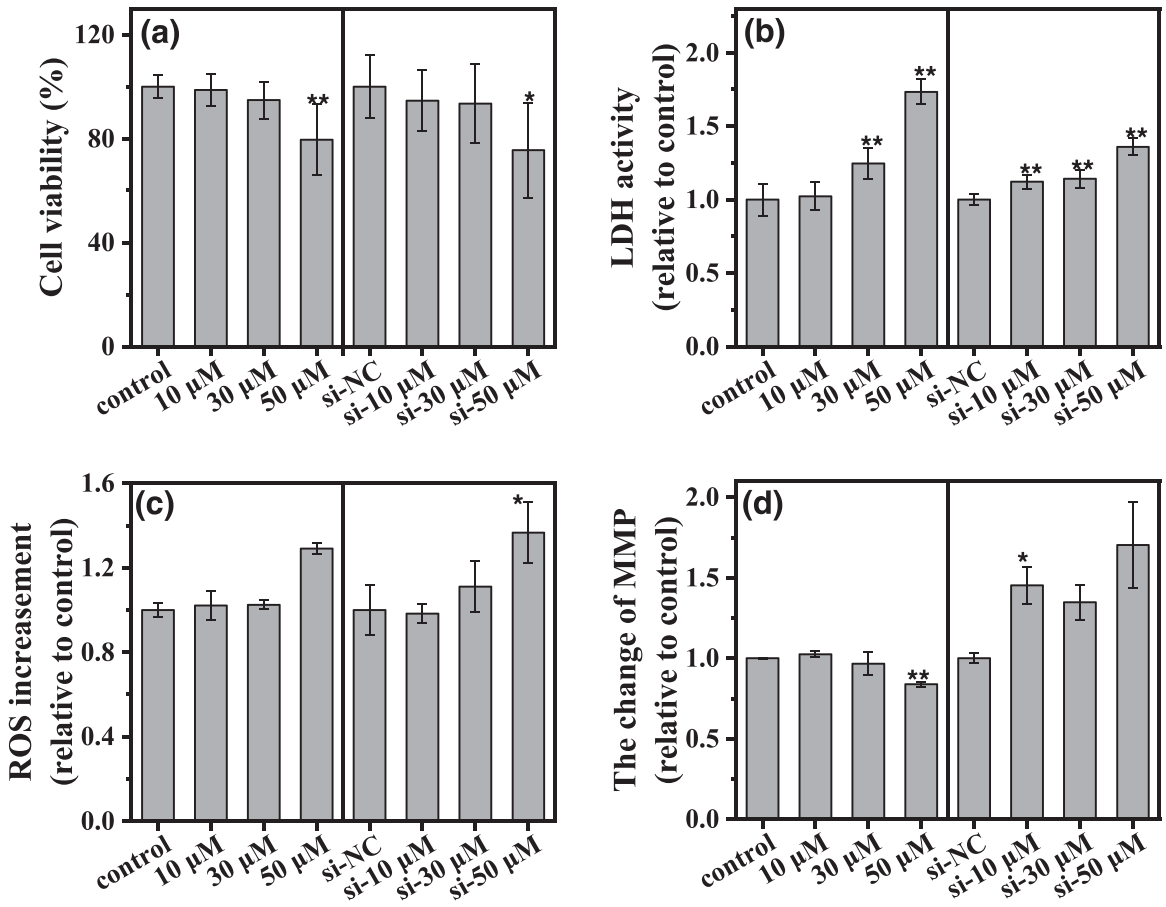

Fig. 4. Methanethiol induced cytotoxicity in 16HBE cells, and influence of si-RNA. Data are presented as the mean ± SD. One-way ANOVA was used for the statistical analyses and $^{*}p < 0.05$, $^{**}p < 0.01$, n = 3, compared with control group.

silencing. Moreover, the extracellular LDH activity decreased after gene silencing, with the activity of LDH in the si-50 μM group being 19% lower than that in the 50 μM group (Fig. 4b). Moreover, no statistically significant change in ROS was found between the normal group and the transfection group (Fig. 4c). However, the MMP of cells in the transfection group increased by 45%, 35%, and 70% under 10, 30, and 50 μM methanethiol exposure, respectively (Fig. 4d). As mentioned above, in the 16HBE cells, methanethiol was metabolized to DMS by METTL7B. Thus, knockdown of METL7B inhibited the methanethiol-mediated rupture of cell membranes and promoted the increase in MMP (Fig. 4d). Furthermore, the decrease in extracellular LDH activity indicates, to a certain extent, that methanethiol and DMS jointly produce toxic effects on the cell. Thus, we demonstrated the metabolic transformation associated with methanethiol in 16HBE cells can affect the cytotoxicity. Besides DMS, other methanethiol metabolites might be produced in the 16HBE cells, but below the detection limit, including some endogenous small molecular substances and exogenous sulfides. Both methanethiol itself and its metabolites have an effect on cytotoxicity and this mechanism of this toxicity is so complicated that it requires further study.

In addition, we performed metabolome analysis of the cell culture medium of the 10 μM exposure group to predict the effect of methanethiol exposure on 16HBE cells. A total of 408 compounds were identified, of which 22 were found to be significantly up-regulated and 3 were significantly down-regulated after simple processing of the metabolomics data (Fig. 5 and S6). Among the identified substances, most were fatty amines, amino acids, peptides, phenols and purines, all of which play important roles in cellular metabolism and intracellular chemical reactions. Thus, exposure to methanethiol affected cellular metabolic responses. Furthermore, these compounds were concentrated in The Small Molecule Pathway Database (SMPDB) and located in the beta-oxidation of very-long-chain fatty acids, vitamin B6 metabolism, methionine metabolism, urea cycle, arginine and proline metabolism, and lysine degradation pathways. The most noteworthy of the above pathways is methionine metabolism because methanethiol is produced by methionine degradation in the human body, and is partly responsible for bad breath and body odor (Tangerman, 2009). Metabolomics experiments detected significant fold changes in adenosine and 5′-S-methylthioadenosine in the 16HBE cells after exposure to methanethiol, which are the main two substances in methionine metabolism. This result also indicates that methanethiol will not only affect its 16HBE cell toxicity but also affect the metabolic process of its upstream substances during its metabolic transformation. Other pathway results also suggested a direction to the metabolic toxicity of methanethiol.

In summary, methanethiol was converted into DMS by thiol S-methyltransferase, possibly with S-adenosyl-L-methionine as the substrate (Fig. 6). The cell necrosis pathway was mainly activated by TNF, which activated the intracellular RIPK1-RIPK3 necrosomes. These two key genes subsequently activated and phosphorylated the downstream mitochondrial-targeted genes CAMKII and MLKL. Thereafter, the permeable conversion channel complexes (ANT, VDAC, CypD) were opened, and then calcium iron overload occurred. At the same time, MLKL could have also caused the activation of PGAM5 on the mitochondrial membrane. In the presence of a large amount of ROS, the MMP decreased or even disappeared, finally leading to cell necrosis (Fig. 6). Furthermore, we found that inhibition of methanethiol biotransformation also affected cell viability, membrane integrity and MMP to some extent. Therefore, this indicates that methanethiol metabolism in 16HBE cells is closely related to its cytotoxicity.

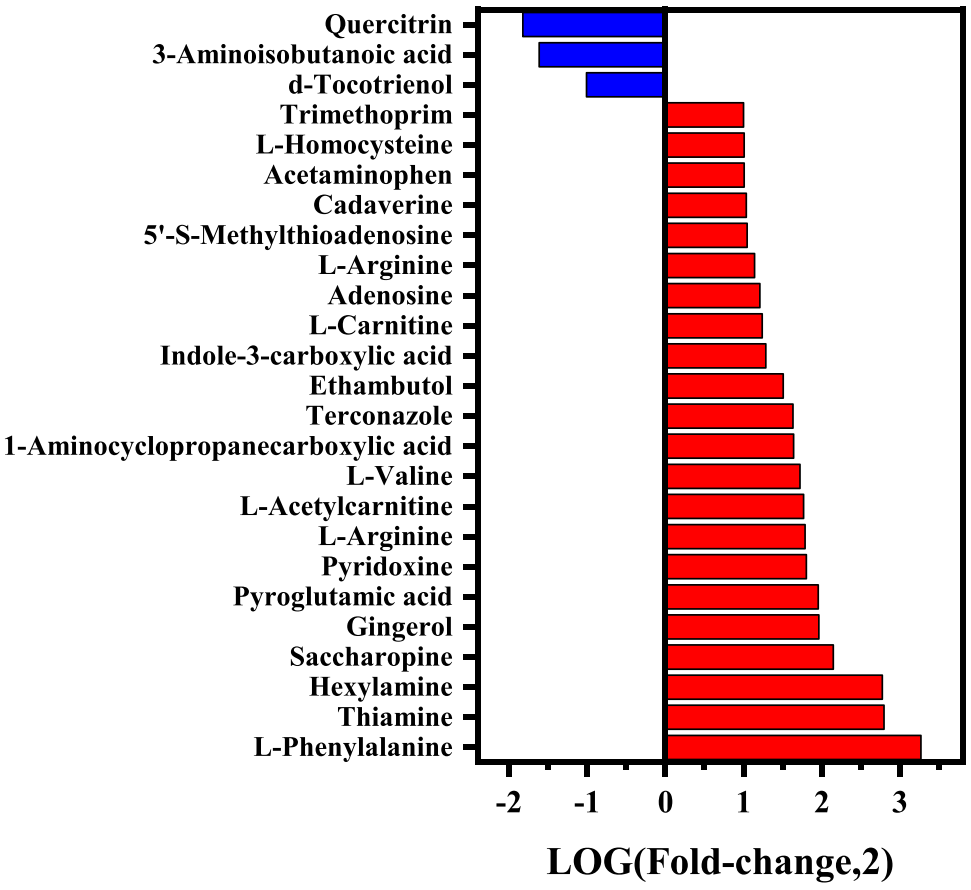

Fig. 5. The metabolomics analysis of medium samples revealed distinct differences in endogenous metabolites between control and exposed with methanethiol in 16HBE cells.

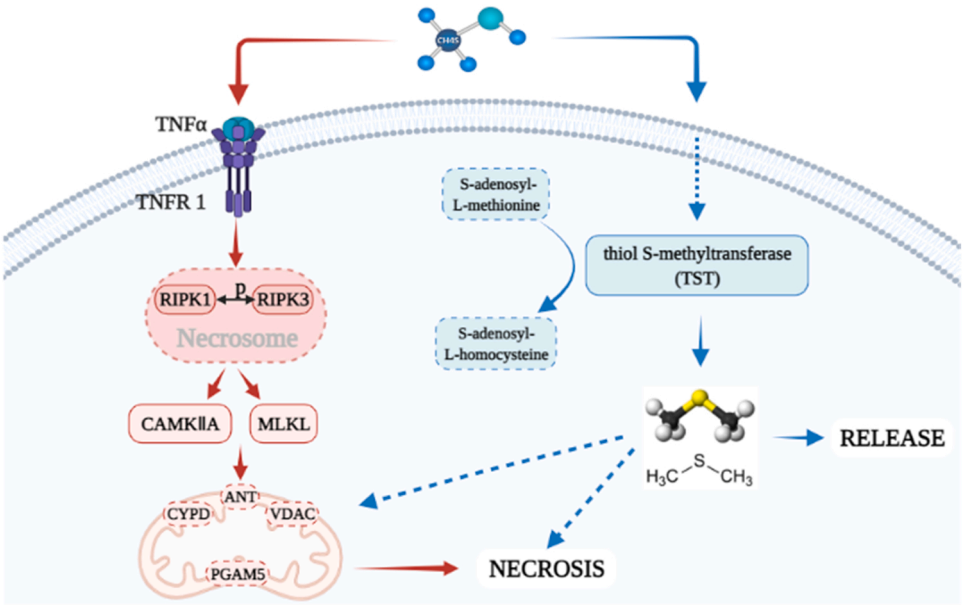

Fig. 6. The pathway of biotransformation and cell necrosis in 16HBE cells with methanethiol exposure.

4. Conclusion

The present study demonstrates that in mammalian cells, methanethiol exposure could be metabolized into DMS, as catalyzed by the METTL7B enzyme. Meanwhile, upregulation of the TNF signaling pathway, as activated by produced intracellular ROS, can eventually cause cell necrosis. During methanethiol-induced cell necrosis, formation of the RIPK1 and RIPK3 necrosome is found to be the key event in this pathway, and destruction of the cellular mitochondrial function is the main target of methanethiol-induced cell necrosis. Nevertheless, our research has not resolved the complete metabolic pathway of methanethiol in 16HBE cells. And the TNF pathway, which recognized as methanethiol-induced cell necrosis is only one aspect of the cell necrosis mechanism. Therefore, further studies into the metabolic mechanism of methanethiol in the human body and its cell damage mechanism are warranted.

CRediT authorship contribution statement

Jinting Lei: Methodology, Formal analysis, Writing – original draft. **Guiying Li:** Writing – review & editing, Supervision. **Hang Yu:** Methodology, Data curation. **Taicheng An:** Conceptualization, Supervision.

Declaration of Competing Interest

The authors declare that they have no known competing financial interests or personal relationships that could have appeared to influence the work reported in this paper.

Acknowledgements

This work was supported by National Key Research and Development Project (2019YFC1804504 and 2019YFC1804503), National Natural Science Foundation of China (41877363 and U1901210), and Local Innovative and Research Teams Project of Guangdong Pearl River Talents Program (2017BT01Z032).

Appendix A. Supporting information

Supplementary data associated with this article can be found in the online version at doi:10.1016/j.ecoenv.2022.113486.

References

Baines, C.P., 2010. Role of the mitochondrion in programmed necrosis. Front. Physiol. 1, 156.
Blaser, H., Dostert, C., Mak, T.W., Brenner, D., 2016. TNF and ROS crosstal in inflammation. Trends Cell Biol. 26 (4), 249–261.
Borchardt, R.T., Cheng, C.F., 1978. Purification and characterization of rat liver microsomal thiol methyltransferase. Biochim. Biophys. Acta 522 (2), 340–353.
Bremer, J., Greenberg, D.M., 1961. Enzymic methylation of foreign sulfhydryl compounds. Biochim. Biophys. Acta 46 (2), 217–224.
Cho, Y., Challa, S., Moquin, D., Genga, R., Ray, T.D., Guildford, M., Chan, F.K.M., 2009. Phosphorylation-driven assembly of the RIP1-RIP3 complex regulates programmed necrosis and virus-induced inflammation. Cell 137 (6), 1112–1123.
Chu, W.M., 2013. Tumor necrosis factor. Cancer Lett. 328 (2), 222–225.
Derr, R.F., Draves, K., 1983. Methanethiol metabolism in the rat. Res. Commun. Chem. Path. Pharmacol. 39 (3), 503–506.
Fang, J., Xu, X., Jiang, L., Qiao, J., Zhou, H., Li, K., 2019. Preliminary results of toxicity studies in rats following low-dose and short-term exposure to methyl mercaptan. Toxicol. Rep. 6, 431–438.
Festjens, N., Vanden Berghe, T., Vandenabeele, P., 2006. Necrosis, a well-orchestrated form of cell demise: signalling cascades, important mediators and concomitant immune response. Biochim. Biophys. Acta-Bioenergetics 1757 (9–10), 1371–1387.
Fleury, C., Mignotte, B., Vayssiere, J.L., 2002. Mitochondrial reactive oxygen species in cell death signaling. Biochimie 84 (2–3), 131–141.
Furuhashi, T., Ishii, R., Onishi, H., Ota, S., 2020. Elucidation of biochemical pathways underlying VOCsproduction in A549 cells. Front. Mol. Biosci. 7, 116.
Glauser, T.A., Kerremans, A.L., Weinshilboum, R.M., 1992. Human hepatic microsomal thiol methyltransferase. Assay conditions, biochemical properties, and correlation studies. Drug Metab. Dispos. 20 (2), 247–255.
Halestrap, A.P., McStay, G.P., Clarke, S.J., 2002. The permeability transition pore complex: another view. Biochimie 84 (2–3), 153–166.
Hamanaka, R.B., Chandel, N.S., 2010. Mitochondrial reactive oxygen species regulate cellular signaling and dictate biological outcomes. Trends Biochem. Sci. 35 (9), 505–513.
He, P., Du, W., Xu, X., Zhang, H., Shao, L., Lu, F., 2020. Effect of biochemical composition on odor emission potential of biowaste during aerobic biodegradation. Sci. Total Environ. 727, 138285.
Jiang, L., Fang, J., Li, K., Xu, X., Qiao, J., 2021. Lung tissue inflammatory response and pneumonocyte apoptosis of SD rats after a 30-day exposure in methyl mercaptan vapor. J. Air Waste Manag. Assoc. 71 (5), 540–552.
Johnson, P.W., Ng, W., Tonzetich, J., 1992. Modulation of human gingival fibroblast cell metabolism by methyl mercaptan. J. Periodontal Res. 27 (5), 476–483.
Lake, B.G., Price, R.J., Walters, D.G., Phillips, J.C., Young, P.J., Adams, T.B., 2003. Studies on the metabolism of the thiofurans furfuryl mercaptan and 2-methyl-3-furanthiol in rat liver. Food Chem. Toxicol. 41 (12), 1761–1770.
Lancero, H., Niu, J., Johnson, P.W., 1996. Exposure of periodontal ligament cells to methyl mercaptan reduces intracellular pH and inhibits cell migration. J. Dent. Res. 75 (12), 1994–2002.
Lin, Y., Choksi, S., Shen, H.M., Yang, Q.F., Hur, G.M., Kim, Y.S., Tran, J.H., Nedospasov, S.A., Liu, Z.G., 2004. Tumor necrosis factor-induced nonapoptotic cell death requires receptor-interacting protein-mediated cellular reactive oxygen species accumulation. J. Biol. Chem. 279 (11), 10822–10828.
Liu, X., Lu, B., Fu, J., Zhu, X., Song, E., Song, Y., 2021. Amorphous silica nanoparticles induce inflammation via activation of NLRP3 inflammasome and HMGB1/TLR4/MYD88/NF-kb signaling pathway in HUVEC cells. J. Hazard. Mater. 404 (Pt B), 124050.
Liu, Y., Li, W., Duan, Y., 2019. Effect of H_2O_2 induced oxidative stress (OS) on volatile organic compounds (VOCs) and intracellular metabolism in MCF-7 breast cancer cells. J. Breath. Res. 13 (3), 036005.
Lu, L., Hu, J., Li, G., An, T., 2021. Low concentration Tetrabromobisphenol A (TBBPA) elevating overall metabolism by inducing activation of the Ras signaling pathway. J. Hazard. Mater. 416, 125797.
Lu, W., Duan, Z., Li, D., Jimenez, L.M.C., Liu, Y., Guo, H., Wang, H., 2015. Characterization of odor emission on the working face of landfill and establishing of odorous compounds index. Waste Manag. 42, 74–81.
Maldonato, B.J., Russell, D.A., Totah, R.A., 2021. Human METTL7B is an alkyl thiol methyltransferase that metabolizes hydrogen sulfide and captopril. Sci. Rep. 11 (1), 4857.
Mao, S.H., Zhuang, G.C., Liu, X.W., Jin, N., Zhang, H.-H., Montgomery, A., Liu, X.T., Yang, G.P., 2021. Seasonality of dimethylated sulfur compounds cycling in north China marginal seas. Mar. Pollut. Bull. 170, 112635.
Meng, J., Zhai, Z.X., Jing, B.Y., Cui, H.W., Wang, G., 2019. Characterization and health risk assessment of exposure to odorous pollutants emitted from industrial odor sources. Huanjing kexue 40 (9), 3962–3972.
Ng, W., Tonzetich, J., 1984. Effect of hydrogen sulfide and methyl mercaptan on the permeability of oral mucosa. J. Dent. Res. 63 (7), 994–997.
Singh, A.K., Chandra, R., 2019. Pollutants released from the pulp paper industry: aquatic toxicity and their health hazards. Aquat. Toxicol. 211, 202–216.
Sinha, D., D'Silva, P., 2014. Chaperoning mitochondrial permeability transition: regulation of transition pore complex by a J-protein, DnaJC15. Cell Death Dis. 5, e1101.
Sivret, E.C., Wang, B., Parcsi, G., Stuetz, R.M., 2016. Prioritisation of odorants emitted from sewers using odour activity values. Water Res. 88, 308–321.
Sun, S., Zhao, Z., Rao, Q., Li, X., Ruan, Z., Yang, J., 2021. BDE-47 induces nephrotoxicity through ROS-dependent pathways of mitochondrial dynamics in PK15 cells. Ecotoxicol. Environ. Safe 222, 112549.
Tangerman, A., 2009. Measurement and biological significance of the volatile sulfur compounds hydrogen sulfide, methanethiol and dimethyl sulfide in various biological matrices. J. Chromatogr. B 877 (28), 3366–3377.
Tansy, M.F., Kendall, F.M., Fantasia, J., Landin, W.E., Oberly, R., Sherman, W., 1981. Acute and subchronic toxicity studies of rats exposed to vapors of methyl mercaptan and other reduced-sulfur compounds. J. Toxicol. Environ. Health 8 (1–2), 71–88.
Tu, X., Xu, M., Li, J., Li, E., Feng, R., Zhao, G., Huang, S., Guo, J., 2019. Enhancement of using combined packing materials on the removal of mixed sulfur compounds in a biotrickling filter and analysis of microbial communities. BMC Biotechnol. 19, 52.
Vahlkamp, T., Meijer, A.J., Wilms, J., Chamuleau, R.A., 1979. Inhibition of mitochondrial electron transfer in rats by ethanethiol and methanethiol. Clin. Sci. 56 (2), 147–156.
Vandenabeele, P., Declercq, W., Van Herreweghe, F., Vanden Berghe, T., 2010. The Role of the kinases RIP1 and RIP3 in TNF-induced necrosis. Sci. Signal. 3 (115), re4.
Vichi, S., Cortes-Francisco, N., Caixach, J., 2013. Determination of volatile thiols in lipid matrix by simultaneous derivatization/extraction and liquid chromatography-high resolution mass spectrometric analysis. Application to virgin olive oil. J. Chromatogr. A 1318, 180–188.

Waller, R.L., 1977. Methanethiol inhibition of mitochondrial respiration. Toxicol. Appl. Pharmacol. 42 (1), 111–117.
Xiong, Y., Li, M., Bai, J., Sheng, Y., Zhang, Y., 2021. High level of METTL7B indicates poor prognosis of patients and is related to immunity in glioma. Front. Oncol. 11, 650534.
Yang, K., Wang, C., Xue, S., Li, W., Liu, J., Li, L., 2019. The identification, health risks and olfactory effects assessment of VOCs released from the wastewater storage tank in a pesticide plant. Ecotoxicol. Environ. Saf. 184, 109665.
Yao, X.Z., Chu, Y.X., Wang, C., Li, H.J., Kang, Y.R., He, R., 2019. Enhanced removal of methanethiol and its conversion products in the presence of methane in biofilters. J. Clean. Prod. 215, 75–83.
Ye, D., Jiang, Y., Sun, Y., Li, Y., Cai, Y., Wang, Q., Wang, O., Chen, E., Zhang, X., 2019. METTL7B promotes migration and invasion in thyroid cancer through epithelial-mesenchymal transition. J. Mol. Endocrinol. 63 (1), 51–61.
Ying, Y., Padanilam, B.J., 2016. Regulation of necrotic cell death: p53, PARP1 and cyclophilin D-overlapping pathways of regulated necrosis? Cell. Mol. Life Sci. 73 (11–12), 2309–2324.
Yun, J., Jung, H., Ryu, H.W., Oh, K.C., Jeon, J.M., Cho, K.S., 2018. Odor mitigation and bacterial community dynamics in on-site biocovers at a sanitary landfill in South Korea. Environ. Res. 166, 516–528.
Zheng, G., Liu, J., Shao, Z., Chen, T., 2020. Emission characteristics and health risk assessment of VOCs from a food waste anaerobic digestion plant: a case study of Suzhou, China. Environ. Pollut. 257, 113546.